

Absorption Spectra of Tellurium Clusters in Solid Argon

Parviz Hassanzadeh, Craig Thompson, and Lester Andrews*

Department of Chemistry, University of Virginia, Charlottesville, Virginia 22901 (Received: March 30, 1992; In Final Form: June 23, 1992)

Tellurium clusters (Te_2 , Te_3 , and two structural isomers of Te_4) have been prepared by passing tellurium vapor through an argon microwave discharge and condensing the effluent onto a 12 ± 2 K cold sapphire window. The Te_2 diatomic and two isomers of Te_4 have also been prepared by passing tellurium vapor through a superheater (800 °C) followed by condensing with excess argon at 12 ± 2 K. Absorption bands at 400 and 440 nm were identified as Te_2 , and the forbidden $X2 \leftarrow X1$ transition between spin-orbit components of the $^3\Sigma_g^-$ ground state of Te_2 was observed in the infrared spectrum at 1984.3 cm^{-1} . A structured absorption band centered at 665 nm is assigned to Te_3 , which is in agreement with the resonance Raman excitation profile. Two absorption bands in the near-infrared region (an unstructured band at 760 nm and a structured band centered at 960 nm) were interconverted upon selective photolysis with band-pass filters. These two bands are assigned to structural isomers of Te_4 similar to those observed for S_4 and Se_4 . New infrared bands at 243, 232, and 224 cm^{-1} are assigned to the 760-, 665-, and 960-nm absorbing species, respectively, on the basis of their similar photolysis and annealing behaviors.

Introduction

Tellurium forms molecular chains and exists in two allotropic forms, amorphous and metallic tellurium.¹ Torsion-effusion studies show that tellurium essentially consists of $\text{Te}_2(\text{g})$ in the temperature range of 593–683 K,² however, a mass spectrometric study has identified smaller quantities of the higher cluster species $\text{Te}_3(\text{g})$, $\text{Te}_6(\text{g})$, and $\text{Te}_7(\text{g})$ at 680 K.³ At higher temperatures near 1000 °C, atomic tellurium $\text{Te}(\text{g})$ becomes more important.¹ The spectroscopy of larger tellurium clusters has not been well-studied.

Te_2 has been characterized by photoionization mass spectrometry,^{4,5} photoelectron,^{6,7} laser-induced fluorescence,⁸⁻¹⁰ and absorption spectroscopic techniques.^{11,12} Diatomic tellurium shows absorption bands between 450 and 520 nm, and emission studies give a ground-state vibrational frequency of 246 cm^{-1} .

To the best of our knowledge, the spectroscopic information on tellurium clusters larger than Te_2 is limited to Te_3 , which has been studied by resonance Raman spectroscopy in solid nitrogen¹³ and by electronic structure calculations.¹⁴ Vibrational and absorption spectra for sulfur^{15,16} and selenium¹⁷ trimers and tetramers have recently been observed in solid argon. In the present work the electronic and infrared absorption spectra of Te_2 , Te_3 , and two isomers of Te_4 in solid argon are reported.

Experimental Section

The vacuum system and chamber for matrix-isolation studies have been described previously.^{15,16} A closed-cycle refrigerator (CTI-Cryogenics, Model 21) with an indicator/controller was used to cool and monitor the temperature of the sapphire window. Spectra were recorded on Cary 17 UV-VIS-NIR and Perkin-Elmer 980 IR absorption spectrometers.

Purified tellurium metal (Fisher Laboratory Chemical) was used as received. A quartz superheater¹⁵ composed of two heating stages was used to produce tellurium clusters. The cell was wound with no. 22 nichrome wire (Hoskins Mfg. Co. Hamburg, MI) and grounded in the middle. About $2/3$ of the back part (sample reservoir) was filled with metallic tellurium powder. The reservoir and the front part were heated via two Variac transformers. The reservoir and the superheater temperatures were monitored by a thermocouple enclosed in a quartz jacket and by an optical pyrometer, respectively. A microwave generator (Ophos Instruments, Inc.; MPG-4389) with an Evenson-Broida cavity was also used to produce tellurium clusters by passing tellurium vapor through an argon discharge. The quartz discharge tube, which has a 1-mm orifice, has been described previously;¹⁶ the tube was kept above 500 °C between the reservoir and the ring seal to prevent condensation of tellurium. The discharged gas stream was condensed at 12 ± 2 K, and spectra were recorded before and after annealing and photolysis with a filtered high-pressure mercury arc lamp (BH6-B, 1000 W).

TABLE I: Electronic Absorptions (nm) Observed for Tellurium Clusters in Solid Argon at 12 ± 2 K

obsd bands	assignmt	obsd bands	assignmt
975.0	Te_4	670.0	Te_3
961.0	Te_4	663.0	Te_3
948.0	Te_4	656.5	Te_3
760	Te_4 (broad)	650.0	Te_3
705.0 ^a	Te_3	440	Te_2 (B \leftarrow X)
695.5	Te_3	400	Te_2 (A \leftarrow X)
686.5	Te_3	295	Te_4 (broad)
678.0	Te_3	255	Te_4

^a Accuracy ± 0.5 nm.

Results

Observations will be presented for superheater and microwave discharge sources of tellurium atoms and clusters.

Superheater. Spectra were recorded at different temperatures for the reservoir and the superheater and different argon flow rates. Temperatures around 370 ± 5 °C for the reservoir (6–10 mTorr vapor pressure)¹ and 800 ± 10 °C for the superheater and an argon flow rate of 2 mmol/h gave the best spectra. After sample deposition for 1 h, the UV-visible-near-IR spectrum showed a structured band around 960 nm, a broad, unstructured band centered at 760 nm, two bands at 440 and 400 nm, and two other bands at 295 and 255 nm (Figure 1a). The observed bands are also collected in Table I. The 960- and 760-nm bands were photolyzed selectively with mercury arc band-pass radiation. Combination of water, pyrex glass, red glass, and CS-756 glass provided an 850–1000-nm light source (A), and combination of water, pyrex glass, red glass, and KG5 glass gave a 630–770-nm light source (B). The spectra after alternating photolyses with the filtered light sources A and B and annealing at 40 ± 2 and 50 ± 2 K are shown in Figure 1. As can be seen from the spectra, the structured 960-nm band decreased upon photolysis using source A while the unstructured 760-nm band increased (Figure 1b). Subsequent photolysis using the filtered light source B caused the 760-nm band to decrease and the 960-nm band to increase (Figure 1c). Upon further consecutive photolyses with the filtered light sources A and B, the 960- and 760-nm bands were interconverted (Figure 1b–g). Intensities of the bands at 255 and 295 nm also changed; the 295-nm band followed the changes observed for the 760-nm band. The 400- and 440-nm bands were not affected by photolysis with either A or B radiation sources. Annealing at 40 ± 2 and 45 ± 2 K (Figure 1h) caused the 255-, 295-, and 760-nm bands to increase while the 400-, 440-, and 960-nm bands decreased. All the bands vanished upon further annealing at 50 ± 2 K (Figure 1i). In other experiments where the 960-nm band was weak, it grew on annealing.

In another experiment, the infrared spectrum was recorded from 180 to 2000 cm^{-1} ; this spectrum revealed a sharp new band at

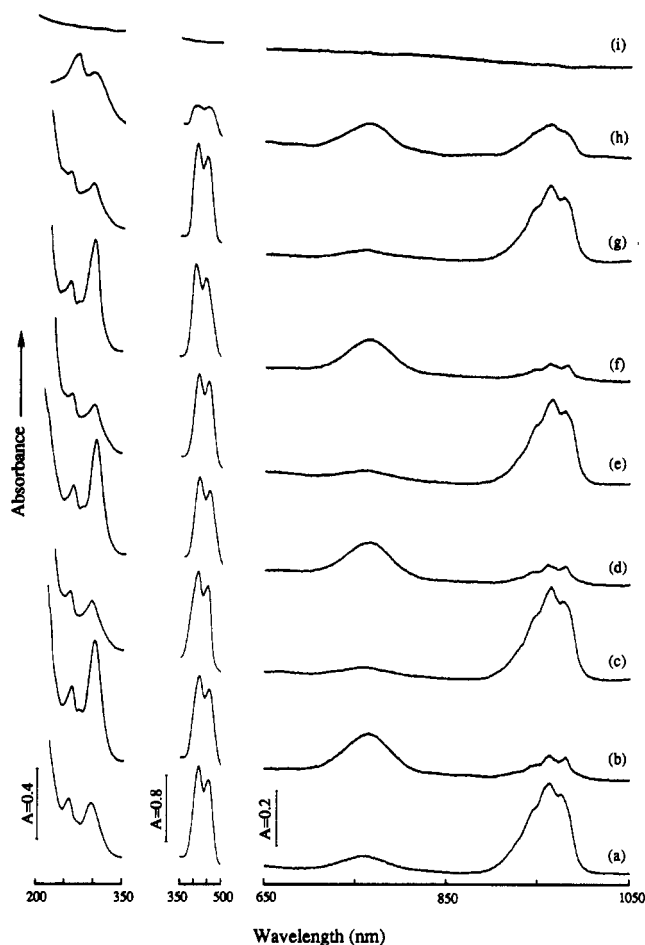


Figure 1. Electronic absorption spectra of superheated tellurium vapor condensed with excess argon at 12 ± 2 K: (a) spectrum after 1 h of sample deposition; (b-g) spectra after consecutive photolysis with 850–1000- and 630–770-nm light sources, respectively; (h) spectrum after annealing at 40 ± 2 K; (i) spectrum after annealing at 50 ± 2 K.

1984.3 cm^{-1} (full-width at half-absorbance maximum, fwhm = 3.0 cm^{-1} , absorbance, $A = 0.21$) and two new weaker bands at 243 cm^{-1} (fwhm = 4.6 , $A = 0.07$) and 224 cm^{-1} (fwhm = 4.2 , $A = 0.02$).

Discharge. Tellurium vapor was mixed with argon, passed through a microwave discharge, and deposited onto a 12 ± 2 K window. The reservoir was heated to 370 ± 5 °C, and a blue discharge extended all the way to the tip of the discharge tube. A green emission due to the excitation of Te_2 by the discharge radiation was readily observed on the window. After 15 min of sample deposition the matrix appeared yellow and gradually changed into yellowish red after 1 h of sample deposition. On longer deposition a deep red matrix was formed. Several spectra were obtained at different stages of deposition, and 1-h deposition was found to give the best spectral quality. Such a spectrum showed two bands at 400 and 440 nm with intensities of ~ 3 absorbance units, a structured band centered at 665 nm, and weaker bands at 760 and 960 nm. The background above 350 nm was so high that the ultraviolet spectrum could not be recorded. The spectrum between 550 and 1050 nm is shown in Figure 2b and contrasted with the spectrum obtained from the superheater experiment (Figure 2a). A high-resolution spectrum of the 665-nm band (Figure 3) showed eight peaks, which are collected in Table I. The 665-nm structured band was not affected by photolysis with a long-wavelength pass filter ($\lambda > 630$ nm) and the full arc ($\lambda > 220$ nm); however, the vibronic structure on the band became slightly sharper. A green emission was observed when the matrix was annealed above 30 ± 2 K. Upon annealing at 35 ± 2 K, the structured bands around 665 and 960 nm increased by 30% and 50%, respectively; the weak 760-nm band showed minimal change. Annealing at 40 ± 2 K caused the 665-nm band to decrease by 5% while the 960-nm band vanished. Further annealing above

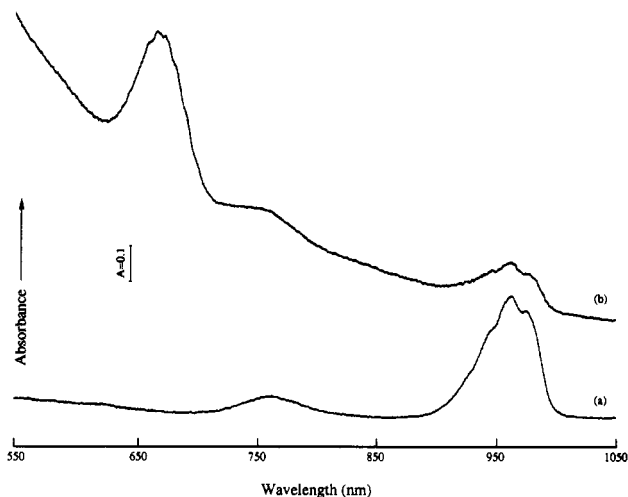


Figure 2. Electronic absorption spectra of tellurium clusters prepared (a) from condensation of superheated tellurium vapor with excess argon on a 12 ± 2 K sapphire window and (b) from a tellurium vapor/argon discharged stream trapped to a 12 ± 2 K sapphire window.

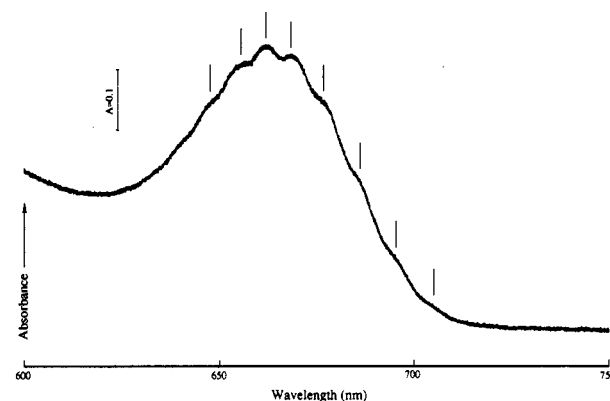


Figure 3. Expanded-scale electronic absorption spectrum in the 600–750-nm region observed from the tellurium vapor/argon discharged stream deposit at 12 ± 2 K.

40 ± 2 K caused all the bands to decrease.

In another series of experiments an intense blue tellurium/argon discharge stream was condensed on a cold CsI window for 10–15 h, and infrared spectra were recorded before and after photolysis with the filtered light sources A and B and annealing at 30, 40, 50, and 55 K. The spectra were similar to those observed with the superheater: a sharp band at 1984.3 cm^{-1} and two bands at 243 and 224 cm^{-1} (Figure 4a). The 224-cm^{-1} band decreased by 12% on photolysis with the light source A while the 243-cm^{-1} band increased by 30% (Figure 4b). Opposite behavior was observed on photolysis with the light source B; that is, the 224-cm^{-1} band increased by 7% while the 243-cm^{-1} band decreased by 15% (Figure 4c). These photoconversions were repeated several times; the 1984.3-cm^{-1} band was not affected (Figure 4d,c). A new band appeared at 232 cm^{-1} on annealing at 40 K, grew further at 50 K, and decreased at $T > 55$ K. The 224-cm^{-1} band decreased on annealing at 40 K and vanished at 50 K. The 243-cm^{-1} band increased at 40 K and decreased gradually at 50 and 55 K.

Discussion

Small tellurium clusters trapped in solid argon will be identified through different methods of preparation, photochemistry, and annealing studies.

Te_2 . The 440- and 400-nm bands were observed in both the superheater and discharge experiments in relatively higher yield than all the other bands studied between 200 and 1200 nm. These bands were not affected by the filtered and unfiltered high-pressure mercury arc irradiation. However, they decreased on annealing at 40 ± 2 and 45 ± 2 K. The 440- and 400-nm bands are assigned to the $A \leftarrow X$ and $B \leftarrow X$ absorptions of Te_2 . These band maxima are to the blue of the origins at 521 and 462 nm, respectively,

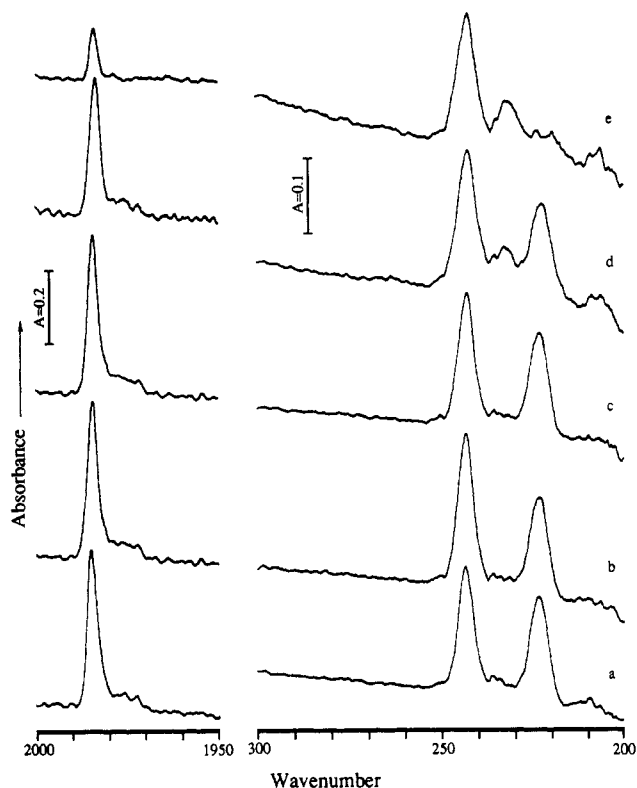


Figure 4. Infrared absorption spectra of tellurium vapor/argon stream deposited on a 12 ± 2 K CsI window: (a) spectrum after 12 h of sample deposit; (b) spectrum after 1-h photolysis with 850–1000-nm light (filter A); (c) spectrum after 1-h photolysis with 630–770-nm light (filter B); (d) spectrum after annealing at 40 ± 2 K; (e) spectrum after annealing at 50 ± 2 K.

determined from the argon matrix emission spectrum.⁹

The 1984.3-cm^{-1} infrared band is assigned to the forbidden $X2 \leftarrow X1$ transition between spin-orbit components of the $3\Sigma_g^-$ ground-state Te_2 molecule. This band is a sharp electronic origin without evidence of broadening due to the distribution of tellurium isotopes in natural abundance. The 1984.3-cm^{-1} band in the argon matrix is blue shifted from the 1974.97-cm^{-1} gas-phase position.⁸ This forbidden transition is observed here owing to a high concentration of Te_2 molecules in the matrix and some degree of asymmetry in the local matrix site. In the case of Se_2 , the analogous transition was observed at 513.9 cm^{-1} in the infrared spectrum, within experimental error of the gas-phase value.¹⁷

Te_4 . The bands at 960 and 760 nm were interconverted upon consecutive photolysis with the filtered light sources A and B, respectively, suggesting that these bands belong to two structural isomers of the same molecular species. A similar interconversion of structural isomers upon selective band-pass irradiation has also been observed for S_4 and Se_4 .^{16,17} These bands are also in the spectral regions expected for Te_4 isomers compared to the unstructured 518-nm and structured 560–660-nm bands of S_4 isomers¹⁶ and the unstructured 633-nm and the structured 710–850-nm bands of Se_4 isomers.¹⁷

The ground-state symmetric stretching vibration for Te_4 is expected to be less than the ground-state fundamental of Te_2 (246 cm^{-1}),⁹ the ground-state symmetric stretching vibration of Te_3 (206 cm^{-1}),¹³ and the present value of $195 \pm 5\text{ cm}^{-1}$ for the excited state ν_1 of Te_3 ; a still lower value is predicted for the excited-state Te_4 fundamental. The spacing between the first and second peaks of the structured 960-nm absorption band is $150 \pm 5\text{ cm}^{-1}$, which is appropriate for a Te–Te vibrational mode. The $150 \pm 5\text{ cm}^{-1}$ interval is assigned to a symmetric vibrational mode in the Te_4 upper state since symmetric modes are most common in vibronic progressions. Furthermore, the $150 \pm 5\text{ cm}^{-1}$ interval is much lower than the ground-state antisymmetric fundamentals to be described below.

Among the bands at 255 and 295 nm, the latter tracks closely with the 760-nm band during these photolyses, suggesting that

the 295- and the 760-nm bands belong to the same species. The 255-nm band, which grows more than the 295-nm band on annealing at 40 ± 2 K (Figure 1h), might belong to a larger tellurium cluster with a cyclic structure.

Infrared spectra reveal three new absorptions at 243, 232, and 224 cm^{-1} whose photolysis and annealing behavior are reasonably related to the absorption bands at 760, 665, and 960 nm accounting for the considerable difference in sample thickness. Photoconversion of the infrared bands at 224 and 243 cm^{-1} with the filtered light sources A and B, respectively, suggests assignment of these bands to the antisymmetric stretching vibrations of Te_4 structural isomers, which were observed at 960 and 760 nm, respectively. The 232-cm^{-1} band, which grows most on annealing, is associated with the Te_3 species to be described next.

Some mention of possible Te_4 structures must be made. The two structural isomers of Te_4 observed here are probably the same as those observed for Se_4 and S_4 .^{16,17} Extensive theoretical studies on S_4 isomers¹⁹ have proposed that the cis-planar structure is the global minimum and that trans-planar, rectangular, and branched-ring structures are low-lying. Experimental observations for S_4 isomers have suggested that the structured red S_4 system is due to the branched-ring isomer.¹⁶ Following the example of S_4 then, the broad 760-nm band is associated with cis-planar Te_4 and the structured 960-nm band with the branched-ring isomer. The two isomers were interconverted upon selective photolysis. Annealing favored the 760-nm-absorbing isomer in the superheater experiments and the 960-nm-absorbing isomer in discharge studies owing to different mechanisms for formation of the different Te_4 isomers. Unfortunately, the present studies cannot identify the more stable isomer.

Te_3 . The new structured band between 650 and 705 nm, observed only in the discharge experiment, is just between the Te_2 and Te_4 absorptions. Due to delocalization of the π electrons the electronic transition energy for a chain molecule is expected to decrease as the chain becomes longer; this suggests that the 665-nm band belongs to Te_3 . The first excited-state vibrational interval of $195 \pm 10\text{ cm}^{-1}$ obtained from the band peaks is less than the 206-cm^{-1} value reported for the ground-state symmetric stretching vibration of Te_3 . This latter value was obtained from a resonance Raman spectrum¹³ of Te_3 in a nitrogen matrix excited at 647 nm, which perfectly matches the present absorption and supports the present Te_3 assignment. The resonance Raman spectrum has been interpreted to indicate a bent Te_3 molecule such as Se_3 , S_3 , and O_3 . The similar structural absorption spectra for S_3 (356–430 nm), Se_3 (480–575 nm), and Te_3 (650–705 nm) further supports the bent geometry for Te_3 .

In the infrared spectrum of the species produced in the tellurium-doped argon discharge, a new band appeared at 232 cm^{-1} after annealing at 40 K and disappeared above 55 K. This band is tentatively assigned to ν_3 of Te_3 . Scaling the fundamental of S_2 (716 cm^{-1}) by the antisymmetric stretching fundamental of bent S_3 (674 cm^{-1}) predicts 231 cm^{-1} for ν_3 of Te_3 , from the fundamental of Te_2 (246 cm^{-1}), in excellent agreement with the observed 232-cm^{-1} value. (On the other hand, a like comparison for triangular S_3 using calculated fundamentals¹⁸ predicts a 153-cm^{-1} fundamental for the possible D_{3h} structure of Te_3 , which could not be observed owing to the 180-cm^{-1} spectrophotometer limit.) We note that the ν_1/ν_3 ratio^{13,16} is 0.89 for both Se_3 and Te_3 and 0.86 for S_3 ,¹⁴ which indicates a decrease in stretch–stretch interaction in the heavier trimer clusters. The vibrational fundamentals observed for Te_3 are appropriate for a C_{2v} structure such as Se_3 , S_3 and O_3 , which is in accord with electronic structure calculations that the bent structure has the lowest energy.¹⁴

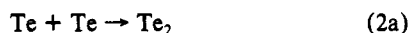
Proposed Reaction Pathways. Reactions occurring in the matrix will be considered for superheater and microwave discharge experiments separately. The microwave discharge and superheater methods of decomposing larger tellurium clusters give slightly different but complementary results.

The absence of Te_3 in the spectrum and the lack of green emission on annealing, which is due to the $\text{Te} + \text{Te}$ recombination in the matrix, suggest that Te_n thermally decomposes mostly into Te_2 (eq 1a) in the present superheater experiments. The Te_4 ,



observed in the initial sample deposit, probably arises from association of Te_2 on deposition although the presence of Te_4 in the superheated vapor cannot be ruled out. The pronounced growth of the 760-nm band on annealing at 40–45 K suggests that Te_4 can be formed from the combination of Te_2 in solid argon (eq 1b).

On the other hand, observation of a strong green emission upon annealing, the high yield of Te_3 , and decrease of higher tellurium clusters in the order of $\text{Te}_2 > \text{Te}_3 > \text{Te}_4$ suggest that the microwave discharge dissociates Te_n into atomic tellurium. Accordingly, tellurium clusters are formed from the consecutive addition reaction of the Te atoms to each other and to Te_2 and Te_3 clusters (eq 2a–c) in the discharge experiment. The optical densities of



Te_3 (665 nm) and Te_4 (960 nm) bands increased on annealing at 35 ± 2 K while the weak 760-nm band showed minimal change. This suggests that Te_3 is formed from the matrix reaction of Te with Te_2 (eq 2b); the same reaction was proposed in the resonance Raman study of Te_3 .¹³

Conclusions

Elemental tellurium vapor has been dissociated by superheating and by microwave discharge, and small tellurium clusters (Te_2 , Te_3 , and two structural isomers of Te_4) have been formed upon condensation with excess argon at 12 ± 2 K. The diatomic cluster Te_2 gave rise to absorption bands at 400 and 440 nm and the forbidden transition between spin-orbit components of the ground state at 1984.3 cm^{-1} . The triatomic cluster Te_3 gave a structured 665-nm absorption. Two tetratomic clusters Te_4 were observed

in the near-infrared at 760 and 960 nm and the far-infrared at 243 and 224 cm^{-1} , respectively; these clusters were interconverted by selective photolysis. The 760-nm-absorbing cluster, made by dimerization of Te_2 , is probably the cis-planar structure, while the 960-nm-absorbing isomer, made by adding Te to Te_3 , is probably the branched-ring structure. The matrix cluster chemistry of Te follows closely with the chemistry of Se and S. Similar absorption bands were observed at progressively longer wavelengths with increasing atomic weight, which suggests similar structures for the group 16 triatomic and tetratomic clusters.

Acknowledgment. We gratefully acknowledge financial support from NSF Grant CHE 88-20764 and helpful discussions with G. D. Brabson.

References and Notes

- (1) Mills, K. C. *Thermodynamic Data for Inorganic Sulfides, Selenides and Tellurides*; Butterworth: London 1974.
- (2) Niwa, K.; Sibata, Z. *J. Chem. Soc. Jpn.* **1940**, *61*, 770.
- (3) Bayer, D. ACM student report, Dec 1965, communicated by W. A. Chupka, Argonne National Laboratory, Argonne, IL, Aug 1968.
- (4) Berkowitz, J.; Chupka, W. A. *J. Chem. Phys.* **1969**, *50*, 4245.
- (5) Guyon, P. M.; Berkowitz, J. *J. Chem. Phys.* **1971**, *54*, 1814.
- (6) Berkowitz, J. *J. Chem. Phys.* **1975**, *62*, 4074.
- (7) Streets, D. G.; Berkowitz, J. *J. Electron Spectrosc.* **1976**, *9*, 269.
- (8) Stone, T. J.; Barrow, R. F. *Can. J. Phys.* **1975**, *53*, 1976.
- (9) Bondybey, V. E.; English, J. H. *J. Chem. Phys.* **1980**, *72*, 6479.
- (10) Ahmen, F.; Nixon, E. R. *J. Mol. Spectrosc.* **1981**, *87*, 101.
- (11) Du Parcq, R. P.; Barrow, R. F. *Chem. Commun.* **1966**, 270.
- (12) Barrow, R. F.; Du Parcq, R. P. *Proc. R. Soc., London A* **1972**, *327*, 279.
- (13) Schnockel, H. Z. *Anorg. Allg. Chem.* **1984**, *510*, 72.
- (14) Von Niessen, W.; Cederbaum, L. S.; Terantelli, F. *J. Chem. Phys.* **1989**, *91*, 3582.
- (15) Brabson, G. D.; Mielke, S.; Andrews, L. *J. Phys. Chem.* **1991**, *95*, 79.
- (16) Hassanzadeh, P.; Andrews, L. *J. Phys. Chem.* **1992**, *96*, 6579.
- (17) Brabson, G. D.; Andrews, L. *J. Phys. Chem.*, in press.
- (18) Rice, J. E.; Amos, R. D.; Handy, N. C.; Lee, T. J.; Schaefer, H. F., III; *J. Chem. Phys.* **1986**, *85*, 963.
- (19) Quelch, G. E.; Schaefer, H. F., III; Marsden, C. J. *J. Am. Chem. Soc.* **1990**, *112*, 8719.

Ab Initio Calculations on $\text{Cl}^-(\text{H}_2\text{O})_{14}$ Clusters: Comparison with the Results from Molecular Dynamics Simulations

James W. Caldwell* and Peter A. Kollman

Department of Pharmaceutical Chemistry, University of California, San Francisco, California 94143-0446
(Received: April 6, 1992)

Recently, Perera and Berkowitz have presented molecular dynamics simulations on $\text{Cl}^-(\text{H}_2\text{O})_{14}$ using two models, one additive (TIP4P) and the other nonadditive (POL1). Rather different structures emerged from these simulations, with the POL1 model predicting "Cl⁻ outside" structures to be more favorable, and TIP4P predicting "Cl⁻ inside" to be more favorable. We have carried out ab initio quantum mechanical calculations at the STO-3G, STO-4G(d), 6-31G, 6-31G(d), and 6-31G(d)/MP2 levels on two low energy geometries resulting from each of the molecular dynamics models. At all levels of ab initio theory, the "Cl⁻ outside" model created by POL1 is the lowest in energy with ΔE_0 of -166.4 and -223.7 kcal/mol at 6-31G(d) and 6-31G(d)/MP2, respectively, compared to the average potential energy of -151 kcal/mol found by Perera and Berkowitz.

Introduction

What are the structures and energies of gas-phase ion-water clusters, and how do these compare to those found in aqueous solution? These questions have been of interest and much studied by physical chemists for more than 2 decades.² The prevailing wisdom, which comes from the ideas of transferability of chemical bonding, is that, after the first shell of waters around the ion filled by four to eight water molecules, the ΔE for addition of more water molecules will smoothly approach a liquidlike value as more waters cluster around a central ion.³ Thus one finds breaks in the

$\Delta H/(\text{no. of waters})$ plots at $n = 1$ to 2 waters for $\text{H}^+\text{N}(\text{CH}_3)_3$ and $n = 4$ to 5 for NH_4^+ . However, inferences about the detailed structure around gas-phase ions has not been possible using experimental methods; furthermore, such inferences have been indirect for ionic solutions, where one can only speak of ensembles of structures. Thus, computer simulation methods, carefully calibrated and compared with experiment where possible, have offered the most promising approach for understanding the relationship between energy and structures in these systems. In the case of small ion-water clusters, increases in computer power are